Osteoblast cell response to a CO_2 laser modified polymeric material

D.G. Waugh[1], J. Lawrence[1] and E.M. Brown[2]

[1]School of Engineering, University of Lincoln, Brayford Pool, Lincoln, LN6 7TS, UK

[2]Queen Elizabeth's Grammar School, Horncastle, Lincolnshire, LN9 5AD, UK

Corresponding author:
D.G. Waugh
School of Engineering
University of Lincoln
Brayford Pool
Lincoln
LN6 7TS, UK

Tel: +44 (0) 1522 668891

Email: DWaugh@lincoln.ac.uk

1.0 – Abstract

Lasers are an efficient technology which can be applied for the surface treatment of polymeric biomaterials to enhance insufficient surface properties. That is, the surface chemistry and topography of biomaterials can be modulated to increase the biofunctionality of that material. By employing CO_2 laser patterning and whole area processing of nylon 6,6 this paper details how the surface properties were significantly modified. Samples which had undergone whole area processing followed current theory in that the advancing contact angle, θ, with water decreased and the polar component, γ^P, increased upon an increase in surface roughness. For the patterned samples it was observed that θ increased and γ^P decreased. This did not follow current theory and can be explained by a mixed-state wetting regime. By seeding osteoblast cells onto the samples for 24 hours and 4 days the laser surface treatment gave rise to modulated cell response. For the laser whole area processing, θ and γ^P correlated with the observed cell count and cover density. Owed to the wetting regime, the patterned samples did not give rise to any correlative trend. As a result, CO_2 laser whole area processing is more likely to allow one to predict biofunctionality prior to cell seeding. What is more, for all samples, cell differentiation was evidenced. On account of this and the modulation in cell response, it has been shown that laser surface treatment lends itself to changing the biofunctional properties of nylon 6,6.

Keywords: Laser surface treatment, osteoblast cells, wettability, nylon 6,6, bioactivity.

2.0 – Introduction

On account of the population living longer and biotechnology having the potential to improve quality of life there is an ever increasing interest in this field [1-6]. More times than not there usually has to be a compromise between bulk and surface properties when determining the best polymeric materials to use [7,8]. In most cases the bulk properties are seen more in favour over those surface properties required [8]. As a result of this, surface properties are not sufficient in terms of the level of bioactivity required giving rise to clinical failure of the implant [9]. Leading on from this, there is a necessity of developing a technique to change the surface properties to enhance and predict the cell response.

Through prior research other methods such as plasmas [10-13], photochemical techniques [14-16] and coating technologies [3,17-19] offer the ability to vary the physiochemical properties of the polymer surface without changing the bulk properties. These various techniques have the ability to improve cell growth and adhesion on polymeric biomaterials; however controlled, precise modification is lacking from the methods named. Laser surface treatment offers the ability to vary the physiochemical surface properties simultaneously with considerably more control and accuracy in comparison to the other

possible techniques [20,21]. Furthermore, lasers offer a convenient means of modifying the surface properties of a material without affecting the bulk properties which may already be sufficient for the intended application.

Nylon 6,6, an off-white engineering thermoplastic, is one of the strongest and most abrasive resistant unreinforced nylons. Owed to the material properties nylon 6,6 possesses this polymer has been used for such biological applications as sutures, tracheal tubes and gastrointestinal segments [19]. With regards to orthopaedic applications, it is seen that nylon is not commonly employed due to the hygroscopic nature having a large effect on the mechanical properties over long periods of time [22]. Having said that, the use of nylon 6,6 within this work gives high value experimentally insofar as to ascertain generic factors for polymeric materials which could be used to predict biological cell response. Also, by modifying the surface of polymeric materials it may be possible to identify other biological applications as this will modulate the cell response and biocompatible properties. On account of nylon 6,6 being a relatively inexpensive polymer when compared to other polymer types, identifying other applications for this material would benefit the biological industry by allowing them to implement cheaper, more economic bio-implant materials.

Even though the links between surface wetting and bioactivity appear to be complex, many believe that the wettability characteristics of a material are a potential route by which the material biofunctionality can be predicted [8,23-28]. Many approaches have fallen short for determining a quantitative theory regarding the bioactivity of a material; however, through research it is hoped that one day the role of wettability can be manipulated and used to allow one to predict quantitatively how a material will operate within a given biological environment. This would give numerous benefits scientifically, economically and socially. That is, having the ability to predict how a given material will perform in a biological environment will significantly reduce the need for unnecessary corrective surgery and will lead to a reduction in unnecessary patient discomfort.

On account of the major benefits that laser surface treatment offers to bio-implant technology, this paper details the employment of a CO_2 laser to modify the surface of nylon 6,6 samples. Following on, the osteoblast cell response *in vitro* is discussed with respect to the surface treatment and the laser-modified wettability characteristics with water.

3.0 – Experimental Technique

3.1 – Nylon 6,6 Material

The nylon 6,6 was sourced in 100 mm^2 sheets with a thickness of 5 mm (Goodfellow Cambridge, Ltd). To obtain a conveniently sized sample for experimentation the as-received nylon sheet was cut into 20 mm diameter discs using a 1 kW continuous wave (cw) CO_2 laser (Everlase S48; Coherent, Ltd).

3.2 – CO_2 Laser-Induced Patterning

In order to generate the required pattern with the CO_2 laser system (10 W 48-Series; Synrad Inc.), Synrad Winmark software version 2.1.0, build 3468 was used. The nylon 6,6 samples were held in place using a bracket with a 20.5 mm diameter hole cut into the centre of the bracket. The focal length of the system was 250 mm away from the output facet of the galvanometer which gave rise to a 95 μm spot size beam that was scanned directly across the stationary target material. It should also be noted that the target material and laser system were held in a laser safety cabinet in which the ambient gas was air. Furthermore, an extraction system was used to remove any fumes produced during laser processing.

The laser-induced patterns were trenches with 50 μm spacing (CT50), hatch with 50 μm spacing (CH50), trenches with 100 μm spacing (CT50) and hatch with 100 μm spacing (CH100). In addition, an as-received control sample was used (AR). The applied scan strategies implemented can be seen in Figure 1. For each of the irradiated patterns the laser power was kept constant at 70% (7 W) with a scanning speed of 600 mms^{-1}.

3.3 – CO_2 Laser Whole Area Irradiative Processing

A cw 100 W CO_2 laser (DLC; Spectron, Ltd) was used to scan a 5 mm diameter beam across the target sample with one pass in order to irradiate the test area with an irradiance of 510 Wcm^2. By using a galvanometer, scanning speeds of 150, 100, 75, 50, 25 and 20 mms^{-1} were employed to irradiate six samples with effective fluences of 16.84 (samples CWA17), 25.51 (sample CWA26), 34.18 (sample CWA34), 51.02 (sample CWA51), 102.04 (sample CWA102) and 127.55 (sample CWA128) Jcm^{-2}, respectively. As with the laser-induced patterning experimentation the samples were held in place on an automated z-variable stage and the experimentation was carried out in a laser safety cabinet in which the ambient gas was air.

3.4 – Topography, Wettability Characteristics and Surface Chemistry Analysis

The surface profiles of each sample were determined using a white light interferometer (WLI) (NewView 500; Zygo, Ltd) with MetroPro and TalyMap Gold Software. The WLI was set-up using a ×10 Mirau lens with a zoom of ×0.5 and working distance of 7.6 mm. On account of the software

employed, Sa and Ra roughness parameters were determined for each sample. Ra can be defined as the arithmetic average of the absolute values along a single specified direction and Sa the arithmetic average of the absolute values over the whole of the laser surface treated area.

Each sample was ultrasonically cleaned in isoproponal (Fisher Scientific Ltd.) for 3 minutes at room temperature before using a sessile drop device to determine various wettability characteristics. To ensure that the sample surfaces were dry a specimen dryer (Metaserv, Ltd.) was employed to blow ambient air across the samples. A sessile drop device (OCA20; Dataphysics Instruments, GmbH) was used with relevant software (SCA20; Dataphysics Intrsuments, GmbH) to allow the recent advancing contact angle, θ, for triply distilled water and diiodomethane to be determined for each sample. By starting with a droplet with a volume of 8 µl the advancing θ were achieved by adding 0.5 µl, respectively, for each measurement. It should also be noted here that after each increment addition of liquid the droplet was left to rest for 1 minute to allow for the droplet to stabilise to its equilibrium state. Thereafter the advancing θ for the two liquids were used by the software to draw an OWRK plot to determine the surface energy of the samples. For the two reference liquids the SCA20 software used the Ström *et al* technique (triply distilled water – SFT(total:72.80), SFT(D:21.80), SFT(P:51.00); diiodomethane – SFT(total:50.80), SFT(D:50.80), SFT(P:0.00)) to calculate the surface energy of the material. It should be noted here that ten θ, using two droplets in each instance, were recorded to achieve a mean θ for each liquid and surface.

All samples were analysed using x-ray photoelectron spectroscopy (XPS). This allowed any surface modifications in terms of surface oxygen content to be revealed. Further XPS experimentation details can be found in [26].

3.5 – *In Vitro* Experimentation

Prior to any biological testing being carried out each sample was autoclaved (D-Series Bench-Top Autoclave; Systec, GmbH) to ensure they were sterile. For all biological work undertaken, unless stated, a biological safety cabinet (BSC) (Microflow Class II ABS Cabinet; BioQuell UK, Ltd) was used to create a safe working environment and to provide a clean, sterile environment to manipulate the osteoblast cells.

Normal human osteoblast cells (Clonetics CC-2538; Lonza, Inc.) were initially cultured in a T75 (75 ml) flask by suspending the cells in 19 ml culture medium comprising of 90% eagle minimum essential medium (Sigma-Aldrich, Ltd., UK) and 10% foetal bovine serum (FBS) (Sigma-Aldrich Ltd., UK). The flask was then placed in an incubator and left for 24 hrs. Following this period of

24 hrs the cells were then assessed and the spent media was aspirated before dispensing 15 ml of fresh media and returning the flask to the incubator for three days.

The period of three days allowed the cells to become confluent in the flask providing enough cells for seeding onto the samples. The cells were detached from the flask using 5 ml Trypisn-EDTA (Sigma-Aldrich Ltd., UK) whilst placed in the incubator for seven minutes. Once all cells had become detached 10 ml culture medium was added to neutralize the Trypsin. In order to aspirate the supernatant the cell culture was centrifuged (U-320R; Boeco, GmbH) for five minutes at 200 g. To ensure the cells were ready for seeding they were re-suspended in 10 ml of culture medium and dispensed between the samples in the 6-well plates. This equated to 0.55 ml (2×10^4 cells/ml) for each sample over three well plates, named plates 1, 2 and 3. The well plates were then placed in an incubator for a set period of time. Plate 1 was removed after 24 hrs and plate 2 and plate 3 were removed after four days. Plate 1 and plate 2 were prepared for SEM analysis as will be discussed in Section 3.6 and plate 3 was prepared for counting using an improved neubauer hemacytometer (Fisher Scientific Ltd., UK) by mixing 10 µl of each cell suspension with 10 µl of trypan-blue (Sigma-Aldrich Ltd., UK). In order to harvest the cells for counting, the same procedure used following the three days incubation, described previously, was implemented. To ensure the cells were ready for counting they were re-suspended in 2 ml of culture medium and 2 ml of the trypan-blue was added.

3.6 – Scanning Electron Microscopy of *In Vitro* Samples

In order to view the attached cells using SEM it was necessary to undertake a procedure to produce a sample that was dehydrated ready for Au coating. The samples were initially rinsed with phosphate-buffered saline (PBS) (Sigma-Aldrich, UK) to remove any unattached cells and then adherent cells were fixed using 1.2% glutaraldehyde in water (Sigma-Aldrich, UK) at room temperature for one hour within the BSC. After an hour the glutaraldehyde solution was removed and the fixed cells were washed with PBS prior to carrying out a graded series of ethanol/distilled water mixtures of 50/50, 80/20, 90/10, 95/5, 98/2 and 100/0. Each sample was left in these mixtures for 10 min to ensure dehydration. Once this procedure was carried out, the samples were mounted and sputter coated with Au so that SEM micrographs could be obtained.

In addition to the cell count described in Section 3.5, the cell cover density was determined following both 24 hrs and 4 day incubation. This was done by analysing the cell coverage on each sample using SEM and optical micrographs with the ImagePro software. The optical micrographs were obtained using an up-right optical microscope (Flash 200 Smartscope; OGP, Ltd) with magnifications varying between ×20 and ×100.

3.7 - Statistical Analysis

All statistical analysis was carried out using SPSS 16.0.2 for Windows software (SPSS Inc., USA) in order to analyze the data obtained using one-way ANOVA to obtain F-ratios and significance levels (p). In addition to one-way ANOVA analysis post hoc multiple comparison tests in the form of Scheffe's range tests were performed in order to determine statistic significance between groups in which results are reported at a mean difference significance level of $p<0.05$.

4.0 – Results and Discussion

4.1 – Effects of CO_2 Laser Processing on Topography

4.1.1 – CO_2 Laser-Induced Patterning

Through previous work it has already been identified that the CO_2 laser-material interaction is that of a thermolytical nature, giving rise to melting and re-solidification [29,30]. As a result of this interaction, CO_2 laser-induced patterning of the nylon 6,6 surfaces gave rise to a significant variation in topography when compared to the as-received sample (AR). This becomes more apparent when comparing the as-received sample (see Figure 2) with the laser patterned samples (see Figure 3).

From Figure 2 and Figure 3 it can be deduced that the CO_2 laser-induced patterned samples had considerably rougher surfaces with the largest peak heights being of the order of 2 μm in contrast to the as-received sample (see Figure 2), which had peaks heights of up to 0.2 μm. On account of the increase in peak heights over the CO_2 laser-patterned samples the surface roughness (see Table 1) increased considerably with the largest Sa of 0.4 μm being achieved with the 50 μm hatch sample (CH50) and largest Ra of 0.2 μm for the 100 μm trench sample (CT100). It is worth noting here that the difference in measurements between Ra and Sa can be accounted for by the way in which each measurement is taken. For instance, it has been observed here that the sample with the highest Ra did not have the highest corresponding Sa. This is due to the fact that Ra measurements are taken across a single defined line; whereas, for Sa the measurement is taken as the arithmetic average across the whole assessed area.

4.1.2 – CO_2 Laser Whole Area Processing

It can be seen from Figure 4 that the CO_2 laser whole area processing of the nylon 6,6 gave rise to a significantly modified surface, especially with those samples which had been irradiated with the

largest fluences (samples CWA102 and CWA128). This can be accounted for by more melting taking place arising from the significantly larger temperature rise owed to the large fluences incident on the nylon 6,6 surfaces.

Figure 4 also shows that there was further evidence of considerable melting on account of one being able to identify craters left from evolved gases breaking at the surface. This is especially apparent for sample CWA102 and sample CWA128 which had larger incident fluences (see Figure 4(e) and Figure 4(f)). As given in Table 1, for all samples with the exception of whole area samples CWA17, CWA26 and CWA34 there was a significant increase in the surface roughness in comparison to the as-received sample (AR) which had a roughness of Sa, 0.1μm, and Ra, 0.03 μm. It should be noted that as a result of the fluences being close to that of the threshold, which were used for samples CWA17, CWA26 and CWA34, the surface roughness results obtained for these samples can be seen to be equivalent to that of the as-received sample (AR). On the other hand, it can be seen that the largest increase in surface roughness arose from samples CWA102 and CWA128 with an Sa of 4 and 3 μm, respectively.

4.2 – Effects of CO_2 Laser Processing on Wettability Characteristics

Current theory states that for a hydrophilic material such as nylon 6,6 an increase in roughness and surface oxygen content should bring about a reduction in contact angle, θ [8]. But, Table 1 shows that this is not the case for the CO_2 laser-induced patterned samples as θ had increased by up to 10° even though a maximum increase in Sa was determined to be around 0.5 μm when compared to the as-received sample (AR). As hypothesized previously [29,30], this phenomenon can be explained by the existence of a mixed-state wetting regime [31-34]. That is, the liquid, when in contact with the sample surface, gave rise to a mixture of Wenzel and Cassie-Baxter regimes. So, the induced pattern yielded a water droplet which was held in an intermediate state such that both wetting regimes coexisted. This can be an explanation as to how an increase in θ was observed for the laser patterned samples and them still be hydrophilic. This mixed-state wetting regime can also account for the observed reduction in apparent polar component, γ^P, and apparent total surface energy, γ^T, with γ^P reducing by up to 8 mJm^{-2} and γ^T reducing by up to 7 mJm^{-2} when compared to the as-received sample (AR). Having said that, it should be noted that the transition to a mixed-state wetting regime, in this instance, is not definite but is a likely explanation for the observed increase in θ.

The CO_2 laser whole area processed samples corresponded with current theory such that the reduction in θ arose from γ^P, γ^T and the surface roughness increasing. Furthermore, From Table 1 it is possible to deduce that θ for sample CWA51 increased in comparison to the as-received sample (AR). This could be on account of the presence of a mixed-state wetting regime as mentioned earlier, even though the surface roughness increased, apparent γ^P decreased and surface oxygen content increased. From Table

1, in comparison to the as-received sample (AR) the largest decrease of 13° in θ was found to arise from sample CWA128 which had the largest incident fluence of 128 Jcm^{-2}. This can be attributed to the fact that a considerable increase in surface roughness brought about a more hydrophilic response from the nylon 6,6.

Owed to the fact that the CO_2 laser-induced patterned samples induced a less hydrophilic response; whereas, a more hydrophilic response was observed for the whole area irradiated patterns, it is possible to deduce from Table 1 that surface oxygen content may not have been the main driving force for wettability. This is due to the oxygen content increasing in all instances by up to 2 %at. for the patterned samples and up to 5 %at. for the whole area samples. The rise in surface oxygen content can be attributed to the thermolytical interaction between the nylon 6,6 material and the CO_2 laser giving rise to melting of the nylon surface allowing oxidation to take place.

From Table 1, one can see that θ was an inverse function of both γ^P and γ^T when collating the results for the CO_2 laser-induced patterned samples and CO_2 laser whole area processed samples. This allows one to identify that all samples corresponded to the theory that an increase in surface energy components gave rise to a reduction in θ even though an increase in θ was observed for the CO_2 laser-induced patterned nylon 6,6 samples.

On account of samples with Ra and Sa values slightly higher than the as-received sample (AR) giving rise to an increase in θ of up to 15° it can be said that there was no correlation between the laser-induced roughness and θ. This can be primarily seen to be on account of the CO_2 laser-induced patterned samples in which a mixed-state wetting regime occurred to give an increase in θ even though a reduction in surface energy components and an increase in surface roughness was observed. Therefore, it has been seen in this instance that the topographical surface pattern appeared to be the main driver for the manipulation of the wettability characteristics. What is more, following CO_2 laser whole area irradiative processing an increase in surface roughness, increase in γ^P and γ^T gave rise to a reduction in θ. This further suggests that the induced patterns had a large impact on the wetting regime and wetting characteristics.

4.3 – Effect of CO_2 Laser Processing on Osteoblast Cell Response: 24 Hrs

4.3.1 – CO_2 Laser-Induced Patterning

It can be seen in Figure 5 and Figure 6 that the osteoblast cells had to some extent adhered to the differing surfaces. That is, the cells firstly attached, adhered and had begun to spread across the surfaces. The extent to which this phenomenon took place appeared to be dependent on the laser processing owed to the larger areas of cell coverage after 24 hrs of incubation time. In terms of cell

morphology it was seen that following 24 hrs of incubation the osteoblast cells on both the as-received (see Figure 5) and the CO_2 laser-induced patterned nylon 6,6 samples (see Figure 6) were bipolar in nature apart from the 100 μm trench samples (see Figure 6(b) which were at a more advanced stage of cell growth. What is more, Figure 6 highlights that the CO_2 laser-induced patterning did not give rise to any directionality owed to the fact that the cells grew in random directions.

4.3.2 – CO_2 Laser Whole Area Processing

Figure 7 shows that after 24 hrs of incubation the osteoblast cells had begun to adhere and proliferate across the nylon 6,6 surface following CO_2 laser whole area processing. Similar to the as-received sample (see Figure 5) the morphologies of the cells shown in Figure 7 were equivalent such that, in general, they were bipolar in nature. On the other hand, in addition to bipolar shapes, those cells shown in Figure 7(b) and 7(c) also indicate a clumped cell morphology. This indicates that the different fluences used for the CO_2 laser whole area processing lead to modulation in cell signaling. It should also be noted that those samples irradiated with high fluences of 102 and 128 Jcm^{-2} (CWA102 and CWA128) hindered osteoblast cell response owed to the fact that the cells had covered less area of the samples studied. For samples CWA102 and CWA128 it was found through wettability characteristic analysis that the surface had become more hydrophilic and could suggest that by making the nylon 6,6 surface too hydrophilic, osteoblast cell response was hindered. That is, materials that are too hydrophilic are well known for their cell-repellant properties and hinder the initial protein adsorption needed for a positive cell response [1,35]. Another aspect that should be taken into consideration is that samples CWA102 and CWA128 were irradiated with high fluences (102 and 128 Jcm^{-2}) and as such 'over-melting' would likely have occurred, allowing toxic elements to form at the surface [36]. These evolved toxic substances could have been present on the surface on account of the rapid heating and cooling, trapping these substances until they leached out into the cell media. This would have had a considerable deleterious effect on the osteoblast cell growth as it has been shown that CO and HCN affect cell growth and proliferation [37].

4.3.3 – Wettability Characteristics and Surface Parameters

With regards to the osteoblast cell response in relation to θ, it can be seen from Figure 8 that the CO_2 laser-induced patterned nylon 6,6 samples did not give rise to values of θ which could be correlated with the observed osteoblast cell response. Yet, from Figure 8 it can be seen that θ could play a role in determining the osteoblast cell response to the CO_2 laser whole area processed nylon 6,6. This is on account of the cell cover density increasing as θ increased over samples CWA17, CWA26, CWA34 and CWA51; whereas samples CWA102 and CWA128, which gave rise to reductions in θ gave rise to a hindered cell response giving considerably lower cell cover densities. Also, with samples CWA17

and CWA26 giving rise to similar θ to that of the as-received (AR) sample the cell cover density was seen to be equivalent for these three samples at approximately 20%. As a direct result of this, low fluences had a negligible effect on cell response in comparison to the as-received sample (AR). It is worth remarking here that one of the main differences between the CO_2 laser-induced patterned and CO_2 laser whole area processed nylon 6,6 samples is that a difference in wetting regime has been proposed to explain the difference in wettability characteristics observed. As a result, this transition in wetting regime for the CO_2 laser-induced patterned samples may have had a large impact on the osteoblast cell response of the nylon 6,6 samples. For instance, if the cell media was to have formed air gaps between some of the solid-liquid interface then the cells would not have been able to come into contact with the whole of the nylon 6,6 surfaces and would have had a large impact upon the results obtained.

Figure 8 also shows the relationship between the cell cover density and γ^P for all CO_2 laser processed samples. It can be seen that the cell cover density increased as a result of a decrease in γ^P for the CO_2 laser whole area irradiative processed samples. Also, it is significant to note here those samples which gave results that do not correspond to this trend are those results determined for the CO_2 laser-induced patterned nylon 6,6 samples. The transition in wetting regime could be accountable for these erroneous data points as discussed earlier. In addition, Figure 8 allows one to see that there was no particular correlation between the measured cell cover density and γ^T for any of the CO_2 laser processed samples. This is due to the cell cover density being erratic when correlated with γ^T. On account of this, γ^T was not a dominant parameter in determining the osteoblast cell response to the nylon 6,6 samples.

In terms of the surface oxygen content, it can be seen from Figure 8 that the CO_2 laser-induced patterned samples did not show any trend in terms of measured cell cover density and the surface oxygen content. On the other hand, Figure 8 shows in general that an increase in surface oxygen content for the CO_2 laser whole area processed samples gave rise to an increase in cell cover density until the incident fluence of 51 Jcm^{-2} was exceeded. After 51 Jcm^{-2} it was determined that even though an increase in surface oxygen content had been brought about, a reduction in the cell cover density was observed. It is possible for one to realize that this may not be a direct result of the increase in surface oxygen and could be attributed to the nylon 6,6 becoming too hydrophilic or too toxic on account of the high fluences used as discussed in Section 4.3.2.

It was also observed that there was no correlative relationship between the cell cover densities observed and the surface roughness Ra and Sa for the CO_2 laser processed nylon 6,6 samples. This indicates that the surface roughness was not a dominant surface characteristic to determine the osteoblast cell response to the nylon 6,6 surfaces.

4.3.4 – Statistical Analysis of Osteoblast Cell Response to CO_2 Laser Surface Treated Nylon 6,6 After 24 hrs

With regards to the cell cover density following 24 hrs incubation (See Figure 8), one-way ANOVA analysis showed there was an overall significance for the cell cover density with an F of 26.437 and p of 0.000. Furthermore, a Scheffe's range test indicated that there was statistical difference between the following samples: AR: CT50 and CT100; CT50: CWA17, CWA26, CWA102 and CWA128; CT100: CH50, CWA17, CWA26, CWA102 and CWA128; CH50: CWA102 and CWA128; CH100: CWA17, CWA26, CWA102 and CWA128; CWA34: CWA102 and CWA128; CWA51: CWA102 and CWA128. It was found through the Scheffe's range test that all other sample combinations were not statistically significant.

4.4 – Effects of CO_2 Laser Processing on Osteoblast Cell Response: 4 Days

4.4.1 – CO_2 Laser-Induced Patterning

After 4 days of incubation the cells had grown and proliferated across almost the whole surface of both the as-received sample (see Figure 9) and the CO_2 laser-induced patterned samples (see Figure 10). Another factor which can be taken from Figure 9 and Figure 10 is that the cell morphologies differed between samples; for instance, it was found that the as-received sample (see Figure 9) gave rise to a more coral-like morphology. Sample CT50 (see Figure 10(a)) gave a cell morphology that was more clumped, spindle-like and was growing in a radial nature. Sample CT100 (see Figure 10(b)) was seen to produce a clumped radial cell morphology. Also, it was seen that the two hatch patterns (sample CH50 and sample CH100) (see Figure 10(c) and Figure 10(d)) had cell morphologies which were clumped radial with sample CH50 (see Figure 10(c)) appearing to be more coral-like. This suggests that the different nylon 6,6 surfaces gave to modulation in cell signaling and revealed that this effect occurs following the initial stages of cell adhesion. With this in mind, it is possible for one to see that by having the ability to modulate cell signalling, this type of surface treatment has the potential to be implemented for applications throughout the field of regenerative medicine.

4.4.2 – CO_2 Laser Whole Area Processing

After 4 days of incubation there still was a variation in cell morphologies between some of the whole area processed samples. From Figure 11 it is evident that the cells had rapidly begun to proliferate over the 4 day incubation period such that for all of the samples the cell cover density was tending towards 100% apart from samples CWA102 and CWA128. In fact, sample CWA102 and sample CWA128 had cover densities of 65% and 55%, respectively. This shows that these two CO_2 laser

modified surfaces hindered osteoblast cell response, slowing down the cell growth and proliferation. As suggested previously, this may be because of the nylon 6,6 surfaces for samples CWA102 and CWA128 being too hydrophilic or too toxic on account of toxic elements leaching into the cell media.

In terms of cell morphology Figure 11 shows that the CO_2 laser whole area processed samples gave rise to cell morphologies that were somewhat different. Sample CWA17 (see Figure 11(a)) gave rise to a clumped morphology which was slightly spindle-like. Whereas samples CWA26, CWA34 and CWA51 (see Figures 11(b), (c) and (d) respectively) gave rise to spindle-like morphologies with larger filopodia as the incident fluence increased. Finally, samples CWA102 and CWA128 (see Figure 11(e) and Figure 11(f), respectively) gave rise to morphologies that were similar to that observed after 24 hrs in that the cells were bipolar in nature. The observation of cell differentiation for the CO_2 laser whole area processed samples allows one to identify that there is a likelihood of variations in cell signaling taking place on account of the different surface parameters which have been induced by the CO_2 laser processing. This identifies that CO_2 laser whole area processing of nylon 6,6 has potential to be applied to regenerative medicine applications. In addition to this, it should be noted that it was seen that the cell growth appeared to be more preferential to the craters and cracks which formed during processing indicating that this has a potential to be used for applications which may require selective osteoblast cell growth.

4.4.3 – Wettability Characteristics and Surface Parameters

Figure 12 confirms that the cell cover densities for all samples were tending towards 100% after 4 days of incubation with the exception of sample CWA102 and sample CWA128 . As such, in terms of cell cover density it was not possible to decipher whether or not the different CO_2 laser processing techniques gave rise to a more enhanced osteoblast cell response when compared with the as-received sample. However, a cell count as shown in Figure 12 after the 4 day incubation period provided the opportunity to determine that the affects of the two CO_2 processing techniques on the osteoblast cell response.

It is clear from Figure 12 that there was no correlation between the cell count and θ for the CO_2 laser-induced patterned nylon 6,6 samples which can be accounted for by the transition in wetting regime. In addition, Figure 12 does show that there was a strong correlation between the osteoblast cell response and θ for the CO_2 laser whole area processed samples. That is, for the CO_2 laser whole area processed samples, an increase in cell count was brought about with an increase in θ until a threshold fluence of around fluences just greater than 51 Jcm^{-2}. As a result, this suggests that it is the surface processing technique regardless of the CO_2 laser wavelength that determines the osteoblast cell response of the nylon 6,6 samples. Figure 12 also shows the cell count for the entire CO_2 laser

processed samples in relation to γ^P allowing one to see that there does not appear to be a trend in regards to the CO_2 laser-induced patterned samples and γ^P. In contrast, the CO_2 laser whole area processed samples had a good correlation with γ^P insofar as the cell count steadily decreased for each of the samples upon an increase in γ^P. Furthermore, one can see from Figure 12 that the surface oxygen content did not correlate with the cell count for the CO_2 laser-induced patterned samples. Conversely, it can be seen from Figure 12 that the cell count for the CO_2 laser whole area processed samples increased on account of an increase in surface oxygen content up to sample CWA51 which had an incident fluence of 51 Jcm^{-2}. For those samples which had higher incident fluences (sample CWA102 and sample CWA128) it can be seen that the cell count had dramatically been reduced in comparison to the as-received sample (AR). This is owed to a potential increase in hydrophilicity or surface toxicity as discussed in Section 4.3.3.

There was no distinct correlation between the cell count, γ^T, Ra and Sa. As a result of this it is possible to say that even though no discernible correlation between the cell count and roughness could be determined, the surface roughness could have still played a significant role in cell differentiation as observed through Figures 5 to 7 and Figures 9 to 11. Furthermore, owed to the significant modification in surface roughness on account of both the CO_2 laser-induced patterning and CO_2 laser whole area processing, these techniques could be applied to regenerative medicine.

4.4.4 – Statistical Analysis of Osteoblast Cell Response to CO_2 Laser Surface Treated Nylon 6,6 After 4 Days

In terms of cell cover density following 4 days of incubation one-way ANOVA analysis showed and

overall significance with F being 38.338 and p being 0.000. A Scheffe's range test showed that there

was significance between all samples and sample CWA102 and CWA128. For all other sample combinations there was no statistical difference between them owed to the fact that all samples apart from sample CWA102 and sample CWA128 gave rise to cover densities tending towards 100%.

One-way ANOVA analysis showed that for the cell count following 4 days incubation there was an

overall significance with an F of 51.462 and p of 0.000. By implementing a Scheffe's range test there

was statistical significance between samples AR: CH100 and CWA17; CT50: AR, CT100, CH50, CH100, CWA17, CWA26, CWA51, CWA102 and CWA128; CT100: AR, CWA34, CWA102 and CWA128; CH50: CWA128; CWA17: AR, CWA102 and CWA128; CWA34: CT50 and CWA51. There was no statistical significance determined between any other sample combinations.

5.0 – Conclusions

This work has further shown that CO_2 lasers can be employed in two different optical set-ups to sufficiently modify the surface properties of a polymeric material, namely nylon 6,6. On account of the significant laser-induced surface modifications it was found that the wettability characteristics were somewhat modulated in relation to the technique employed even though the surface roughness had increased for all samples. The samples which had undergone CO_2 laser whole area processing followed current theory in that the contact angle, θ, decreased and the polar component, γ^p, increased in comparison to the as-received sample owed to an increase in surface roughness. On the other hand, for the CO_2 laser-induced patterned samples it was observed that θ increased and γ^P decreased in relation to the as-received sample even though a significant increase in surface roughness was brought about. This did not follow current theory and can be explained by a mixed-state wetting regime in which both Cassie-Baxter and Wenzel regimes are present across the solid-liquid interface.

By seeding osteoblast cells on to the samples for 24 hours and 4 days it was found that the laser surface treatment gave rise to a modulated osteoblast cell response in terms of cell cover density and cell count. It was determined that for the CO_2 laser whole area processing θ and γ^P had some correlation with the observed cell count and cover density. Having said that, for those samples with the largest fluences of 102 and 128 Jcm^{-2} the cell count and cell cover density was dramatically reduced compared to the other samples and can be attributed to an increase in toxicity due to over-melting of the surface. This indicated that a maximum fluence value of around 50 Jcm^{-2} would give rise to the best cell response for the whole area processed samples. It was also found that the laser-induced patterned samples did not give rise to any correlative trend due to the likely wetting regime having a distinct affect on the biomimetic properties of the nylon 6,6.

From the correlations observed within the results one can extrapolate that the CO_2 laser whole area processing technique is more likely to give the opportunity of one being able to predict the biofunctionality of a material prior to cell seeding. What is more, for all samples after four days incubation, cell differentiation was evidenced. With this in mind along with the increase in cell

response one can see that laser surface treatment lends itself to modulating nylon 6,6 biofunctional properties and has the ability to be readily applied to other polymeric materials.

6.0 – Acknowledgements

The authors would like to thank their collaborators: Directed Light Inc., East Midlands NHS Innovation Hub, Nobel Biocare and Photomachining Inc. for all of their much appreciated support. The authors would also like to thank Chemical Engineering, Loughborough University for use of their biological laboratory. This study was financially supported by the EPSRC (EP/E046851/1).

7.0 – References

1. M.S. Kim, G. Khang, H.B. Lee, Gradient polymer surfaces for biomedical applications, Prog. Polym. Sci. 33 (2008) 138-164.

2. M.D. Ball, R. Sherlock, T. Glynn, Cell interactions with laser-modified polymer surfaces, J. Mater. Sci.: Mater. Med. 15 (2004) 447-449.

3. W.Song, Y.K. Jun, Y. Han, S.H. Hong, Biomimetic apatite coatings on micro-arc oxidzed titania, Biomaterials 25 (2004) 3341-3349.

4. K. MacGregor, The Ageing Population: U.K. Focus for Biomedical Engineering - Policy Briefing. The Royal Academy of Engineering 2010.

5. C. O'Connell, R. Sherlock, M.D. Ball, B. Aszalos-Kiss, U. Prendergast, T.J. Glynn, Investigation of the hydrophobic recovery of various polymeric biomaterials after 172nm UV treatment using contact angle, surface free energy and XPS measurements, Appl. Surf. Sci. 255 (2009) 4405-4413.

6. D.F. Williams, On the mechanisms of biocompatibility, Biomaterials 29 (2008) 2941-2953.

7. J. Lawrence, L. Li, Laser Modification of the Wettability Characteristics of Engineering Materials, Professional Engineering Publishing Ltd., Suffolk, UK, 2001.

8. L. Hao, J. Lawrence, Laser Surface Treatment of Bio-Implant Materials, John Wiley & Sons., New Jersey, USA, 2005.

9. J. Black, Biological Performance of Materials: Fundamentals of Biocompatibility; Fourth Edition, CRC Press, Florida, USA, 2006.

10. F. Arefi-Khonsari, M. Tatoulian, F. Bretagonl, O. Bouloussa, F. Rondelez, Processing of polymers by plasma technologies, Surf. Coat. Tech. 200 (2005) 14-20.

11. D. Pappas, A. Bujanda, J.D. Demaree, J.K. Hirvonen, W. Kosik, R. Jensen, S. McKnight, Surface modification of polyamide fibers and films using atmospheric plasmas, Surf. Coat. Tech. 201 (2006) 4384-4388.

12. P.K. Chu, Plasma surface treatment of artificial orthopedic and cardiovascular biomaterials, Surf. Coat. Tech. 201 (2007) 5601-5606.

13. Q. Wei, Y. Liu, D. Hou, F. Huang, Dyanmic wetting behaviour of plasma treated PET fibers, J. Mater. Proc. Tech. 194 (2007) 89-92.

14. R.S. Benson, Use of radiation in biomaterials science, Nucl. Inst. Meth. Phys. Res. B 191 (2002) 752-757.

15. B. Ranby, Surface modification and lamination of polymers by photografting, Int. J. Adhesion. Adhesives 151 (1999) 337-343.

16. B. Ranby, W.T. Yang, O. Tretinnokov, Surface photografting of polymer fibers, films and sheets, Nucl. Inst. Meth. Phys. Res. B 151 (1999) 301-305.

17. E.M. Harnett, J. Alderman, T. Wood, The surface energy of various biomaterials coated with adhesion molecules used in cell culture, Coll. Surf. B 55 (2007) 90-97.

18. F. Milde, K. Goedicke, M. Fahland, Adhesion behaviour of PVD coatings on ECR plasma and ion beam treated polymer films, Thin Solid Films 279 (1996) 169-173.

19. S.R. Paital, N.B. Dahotre, Calcium phosphate coatings for bio-implant applications: Materials, performance factors and methodologies, Mater. Sci. Eng. R 66 (2009) 1-70.

20. C.A. Aguilar, Y. Lu, S. Mao, S. Chen, Direct micro-patterning of biodegradable polymers using ultraviolet and femtosecond lasers, Biomaterials 26 (2005) 7642-7649.

21. W. Pfleging, M. Bruns, A. Welle, S. Wilson, Laser-assisted modification of polystyrene surfaces for cell culture applications, App. Surf. Sci. 253 (2007) 9177-9184.

22. J.J. Rajesh, J. Bijwe, B. Venkataraman, U.S. Tewari, Effect of water absorption on erosive wear behaviour of polyamides, J. Mater. Sci. 37 (2002) 5107-5113.

23. C.J. Van Oss, Energetics of cell-cell and cell-biopolymer interactions, Cell Biochem. Biophys. 14 (1989) 1-16.

24. C.J. Van Oss, C.F. Gillman, A.W. Neumann, Phagocytic Engulfment and Cell Adhesiveness, Marcell Dekker, New York, USA, 1975.

25. D.G. Waugh, J. Lawrence, Wettability and osteblast cell response modulation through UV laser processing of nylon 6,6, App. Surf. Sci. Accepted 08/04/2011.

26. D.G. Waugh, J. Lawrence, The enhancement of biomimetic apatite coatings by means of KrF excimer laser surface treatment of nylon 6,6, Lasers Eng. 21 (2011) 95-114.

27. E.A. Vogler. Role of Water in Biomaterials, in: B.D. Ratner, A.S. Hoffman, F.J. Schoen, J.E. Lemons (eds.), Biomaterials Science: Second Edition, Elsevier Academic Press, San Diego, California, USA, 2004, p. 59.

28. E.A. Vogler, Interfacial Chemistry in Biomaterials Science, Marcel Dekker,New York, USA, 1993.

29. D.G. Waugh, J. Lawrence, D.J. Morgan, C.L. Thomas, Interaction of CO_2 laser-modified nylon with osteoblast cells in relation to wettability, Mater. Sci. Eng. C 29 (2009) 2514-2524.

30. D.G. Waugh, J. Lawrence, C.D. Walton, R.B. Zakaria, On the effects of using CO_2 and F_2 lasers to modify the wettability of a polymeric biomaterial, J. Opt. Laser Technol. 42 (2010) 347-356.

31. X. Chen, T. Lu, The apparent state of droplets on a rough surface, Sci. China Ser. G-Phys. Mech. Astron. 52 (2009) 233-238.

32. S.M. Lee, Th. Kwon, Effects of intrinsic hydrophobicity on wettability of polymer replicas of a superhydrophobic lotus leaf, J. Micromech. Microeng. 17 (2007) 687-692.

33. Y.T. Cheng, D.E. Rodak, Is the lotus leaf superhydrophobic? Appl. Phys. Lett. 86 (2005) 144101/1-144101/3.

34. X. Wu, L. Zheng, D. Wu, Fabrication of superhydrophobic surfaces from microstructured ZnO-based surfaces via a wet-chemical route, Langmuir 21 (2005) 2665-2667.

35. M.C. Lensen, V.A. Schulte, J. Salber, M. Diez, F. Menges, M. Moller, Cellular response to novel, micropatterned biomaterials, Pure Appl. Chem. 80 (2008) 2479-2487.

36. Sigma-Aldrich. Nylon 6,6 Material Safety Data Sheet - Version 3.0. 2008.

37. S.D. Cook, J.P. Ryaby, J.R.N. McCabe, J.J. Frey, J.D. Heckman, T.K. Kristiansen, Acceleration of tibia and distal radius fracture healing in patients who smoke, Clin. Ortho. Rel. Res. 337 (1997) 198-207.

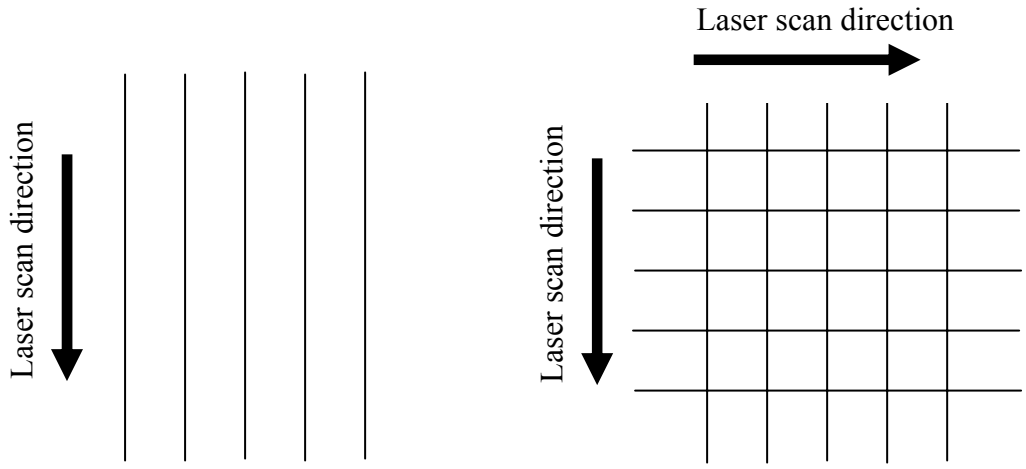

Figure 1 – Diagram showing the scan strategy implemented for (a) the trench and (b) hatch CO_2 laser-induced patterning.

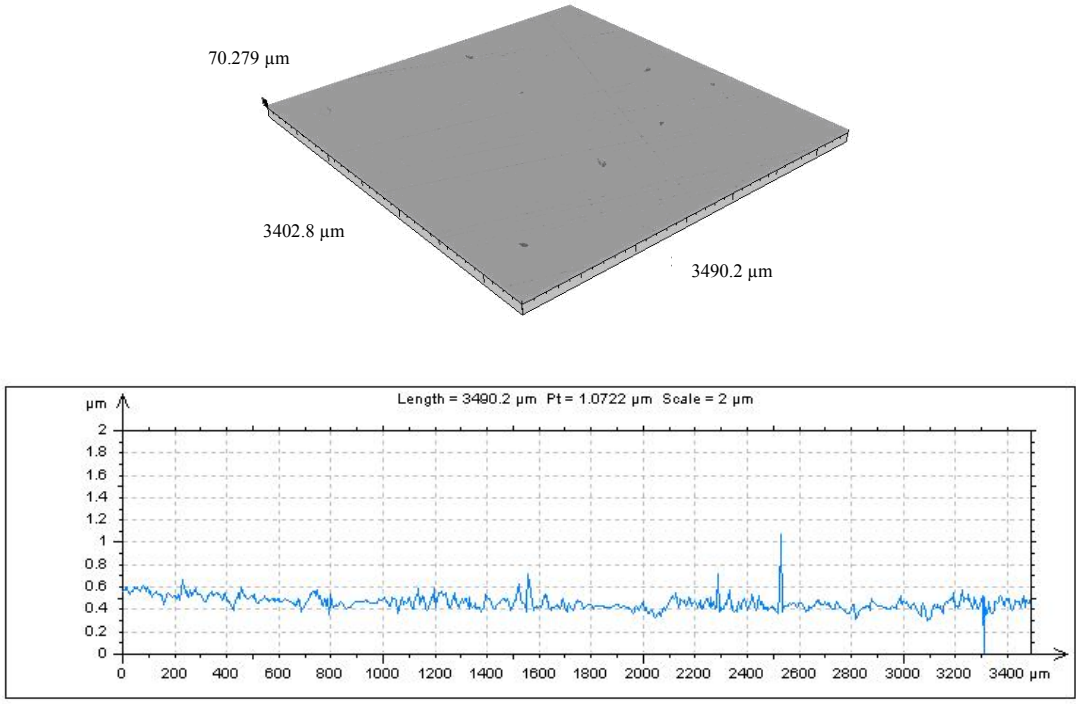

Figure 2 –3-D image and profile extraction for the as-received sample (AR) to showing the surface topography and peak heights prior to laser surface treatment.

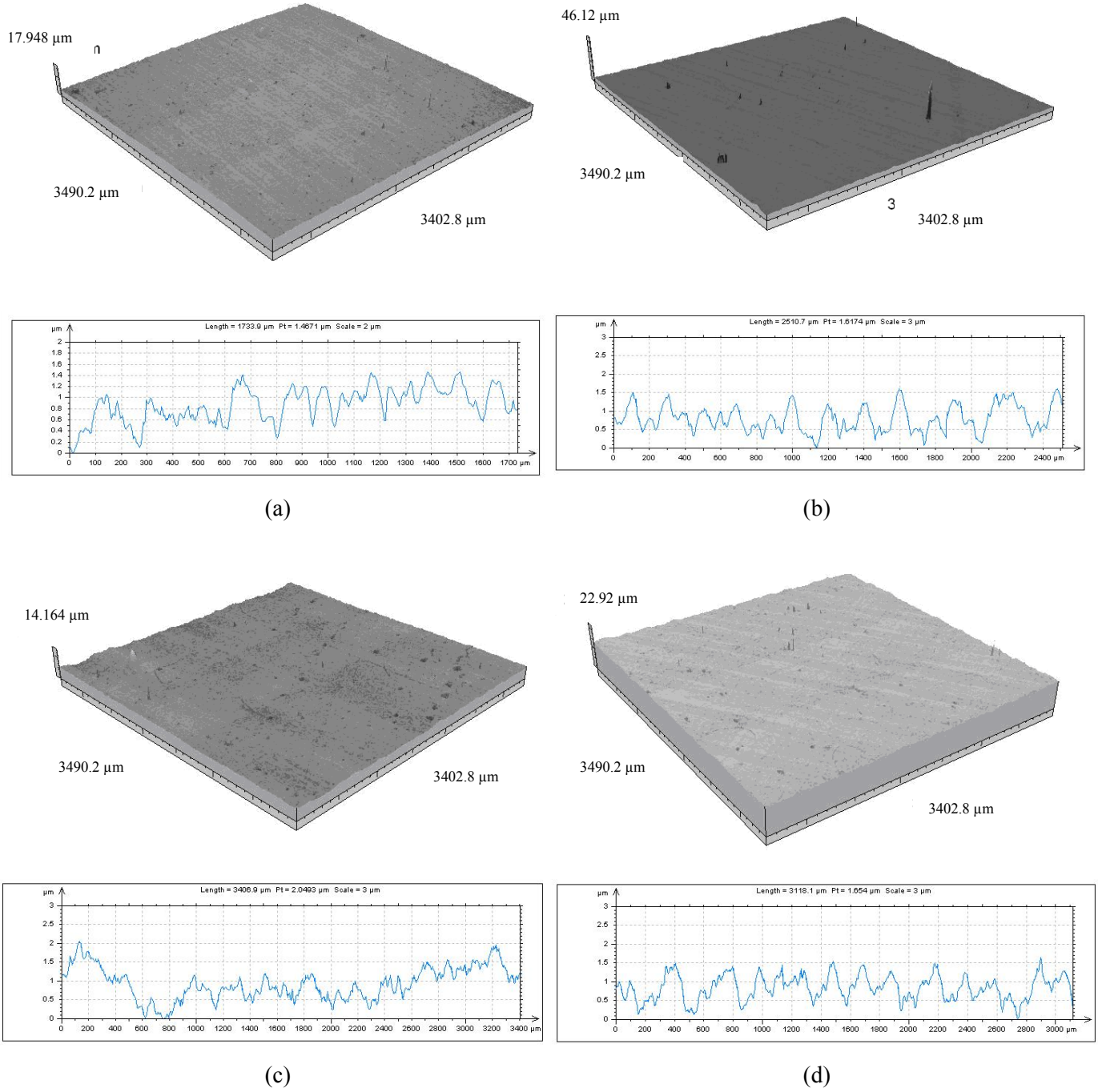

Figure 3 – 3-D images and profile extractions for sample (a) CT50, (b) CT100, (d) CH50 and (d) CH100 showing the surface topographies and peak heights..

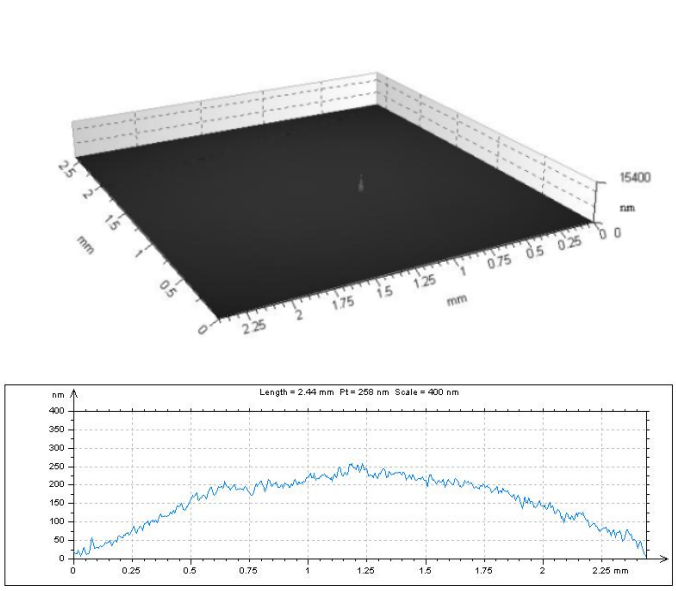
15400
nm
0
mm
Length = 2.44 mm Pt = 258 nm Scale = 400 nm
nm
2.25 mm

(a)

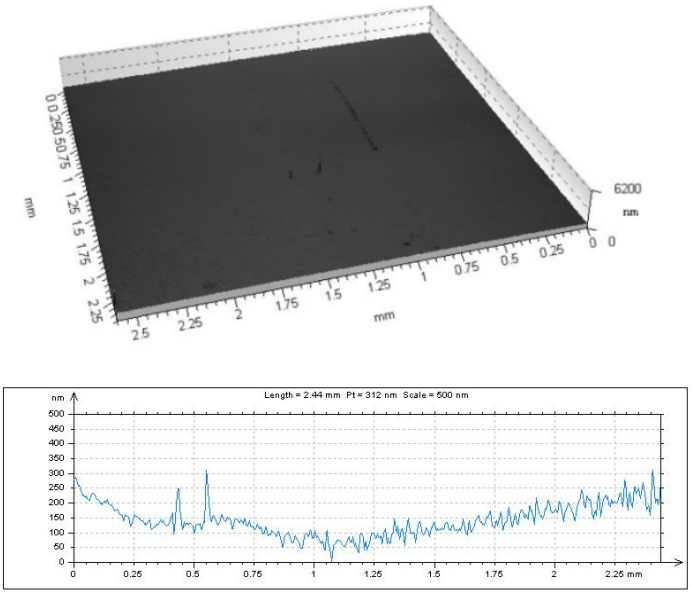
6200
nm
0
mm
Length = 2.44 mm Pt = 312 nm Scale = 500 nm
nm
2.25 mm

(b)

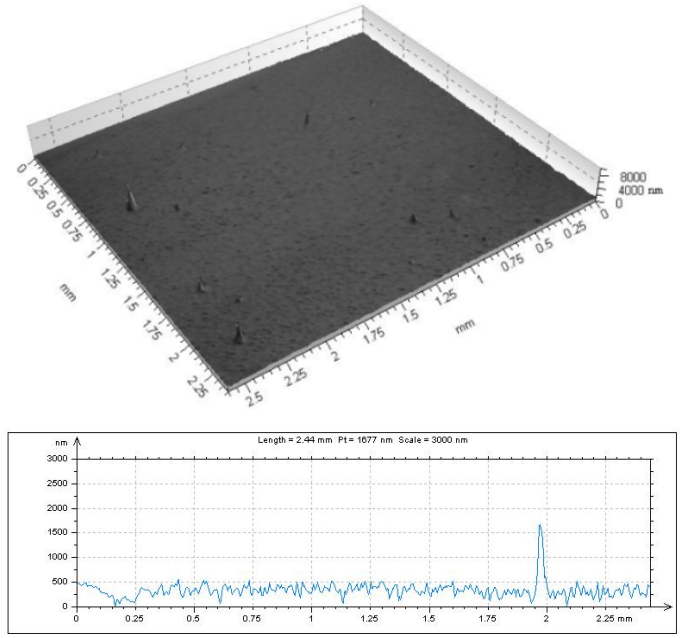
8000
4000 nm
0
mm
Length = 2.44 mm Pt = 1677 nm Scale = 3000 nm
nm
2.25 mm

(c)

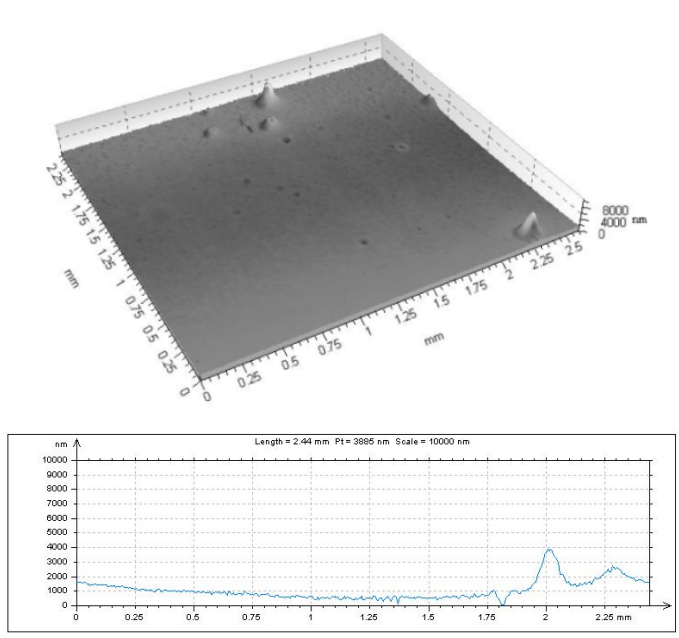
8000
4000 nm
0
mm
Length = 2.44 mm Pt = 3885 nm Scale = 10000 nm
nm
2.25 mm

(d)

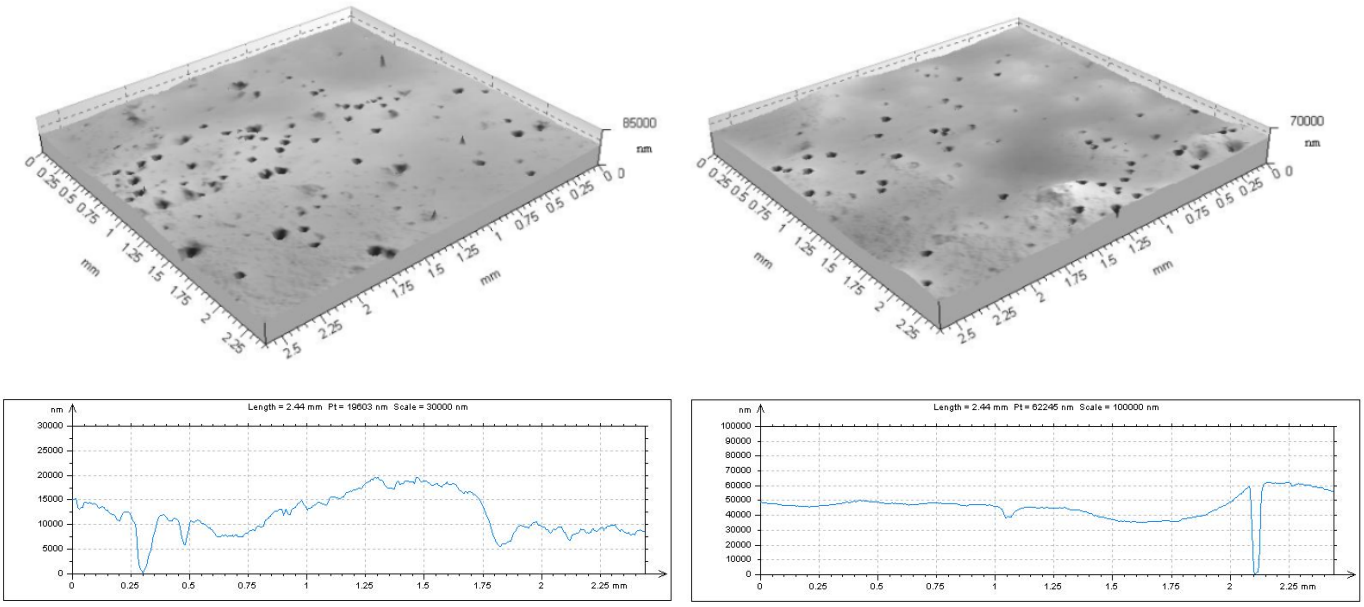

(e) (f)

Figure 4 – 3-D images and profile extractions for sample (a) CWA17, (b) CWA26, (c) CWA34, (d) CWA51, (e) CWA102 and (f) CWA128 showing the surface topography and peak heights.

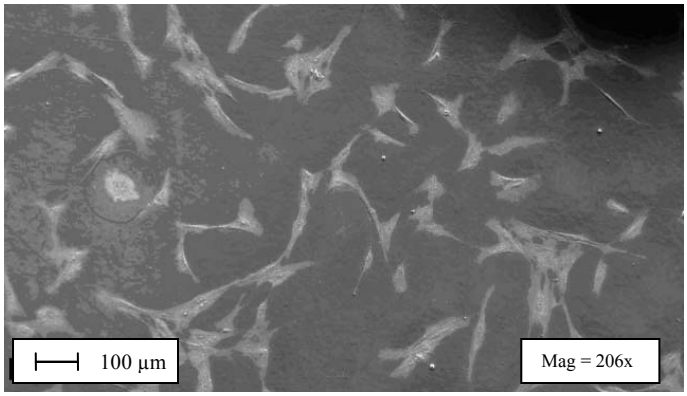

Figure 5 – SEM micrograph of Au coated osteoblast cells on the as-received sample (AR) 24 hrs post seeding.

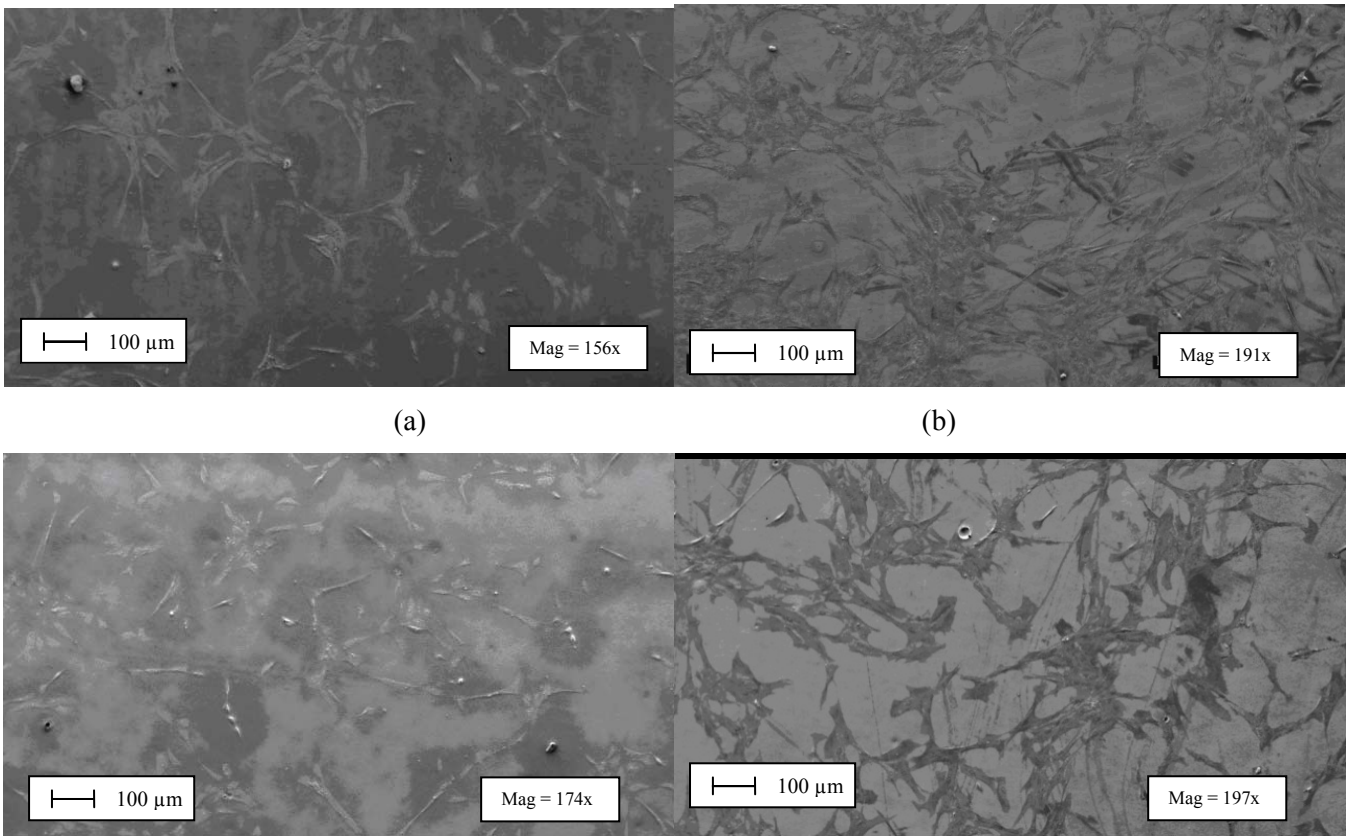

Figure 6 – SEM micrographs of Au coated osteoblast cells on samples 24 hrs post seeding for the CO_2 laser-patterned samples (a) CT50, (b) CT100, (c) CH50 and (d) CH100.

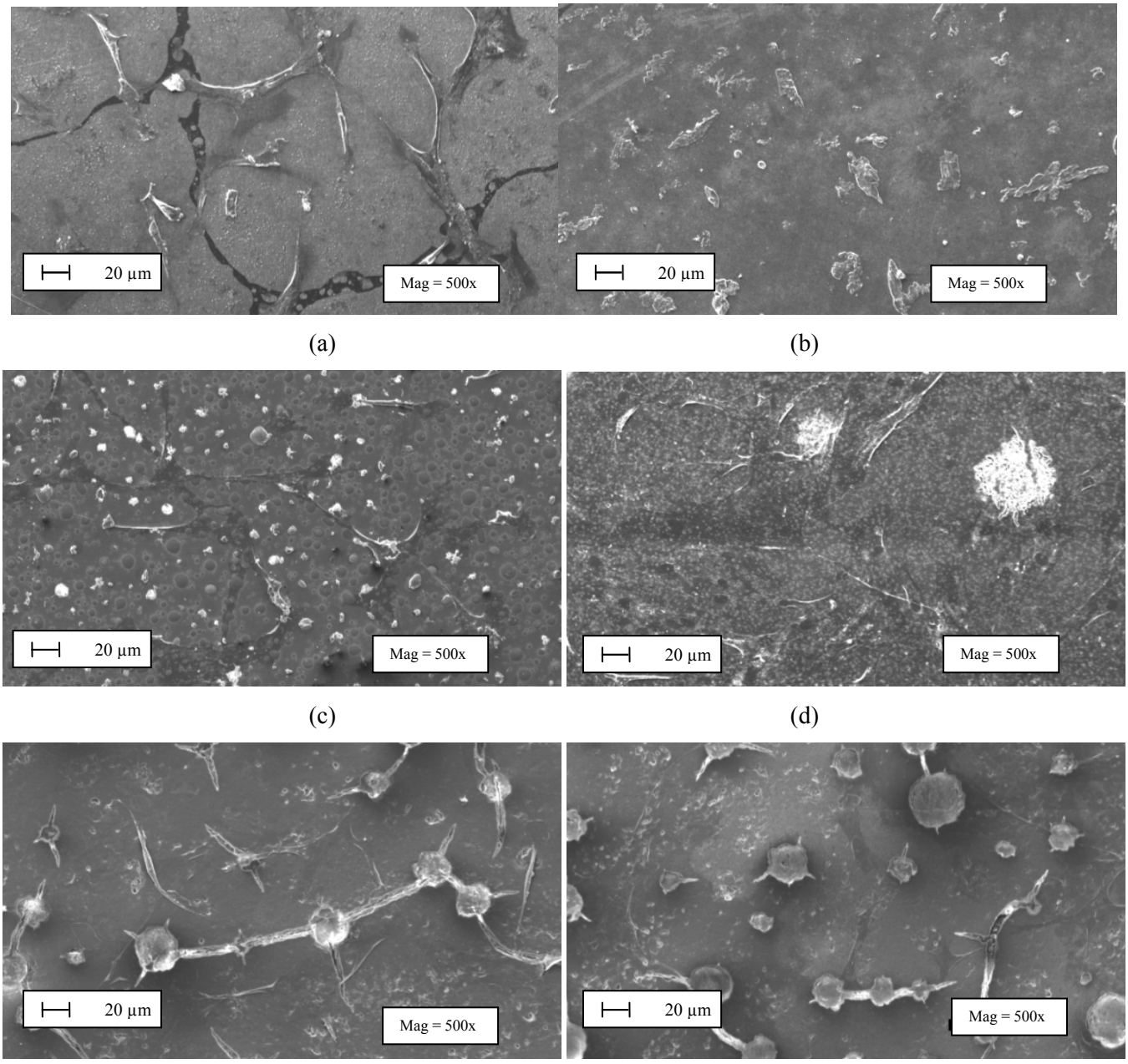

Figure 7 – SEM micrographs of Au coated samples 24 hrs post seeding for the CO_2 laser whole area processed samples (a) CWA17, (b) CWA26, (c) CWA34, (d) CWA51, (e) CWA102 and (f) CWA128.

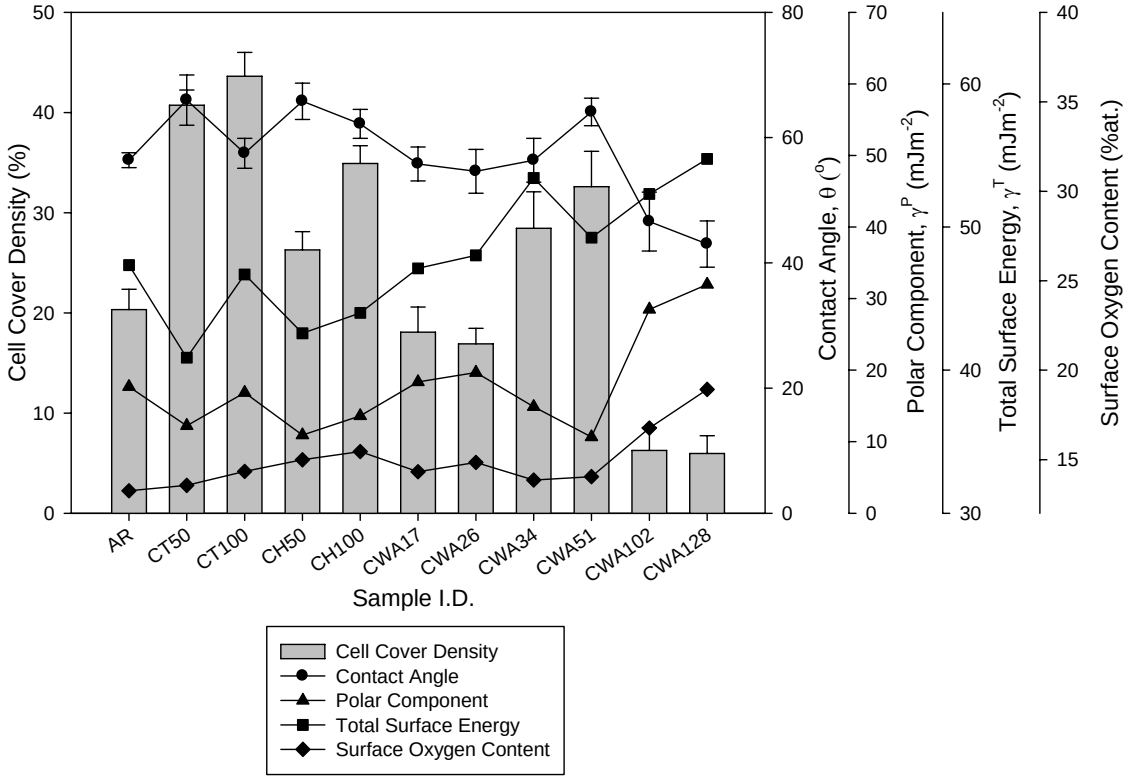

Figure 8 – Histogram showing the cover densities for each of the seeded CO_2 laser processed nylon 6,6 samples after 24 hrs incubation with relation to θ, γ^P, γ^T and surface oxygen content.

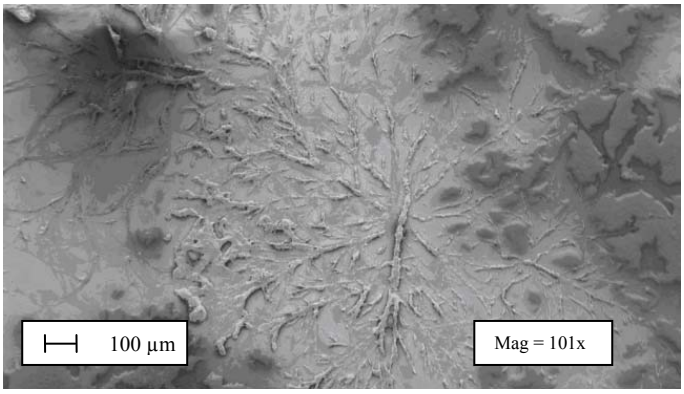

Figure 9 – SEM micrograph of Au coated as-received (AR) sample after 4 days incubation.

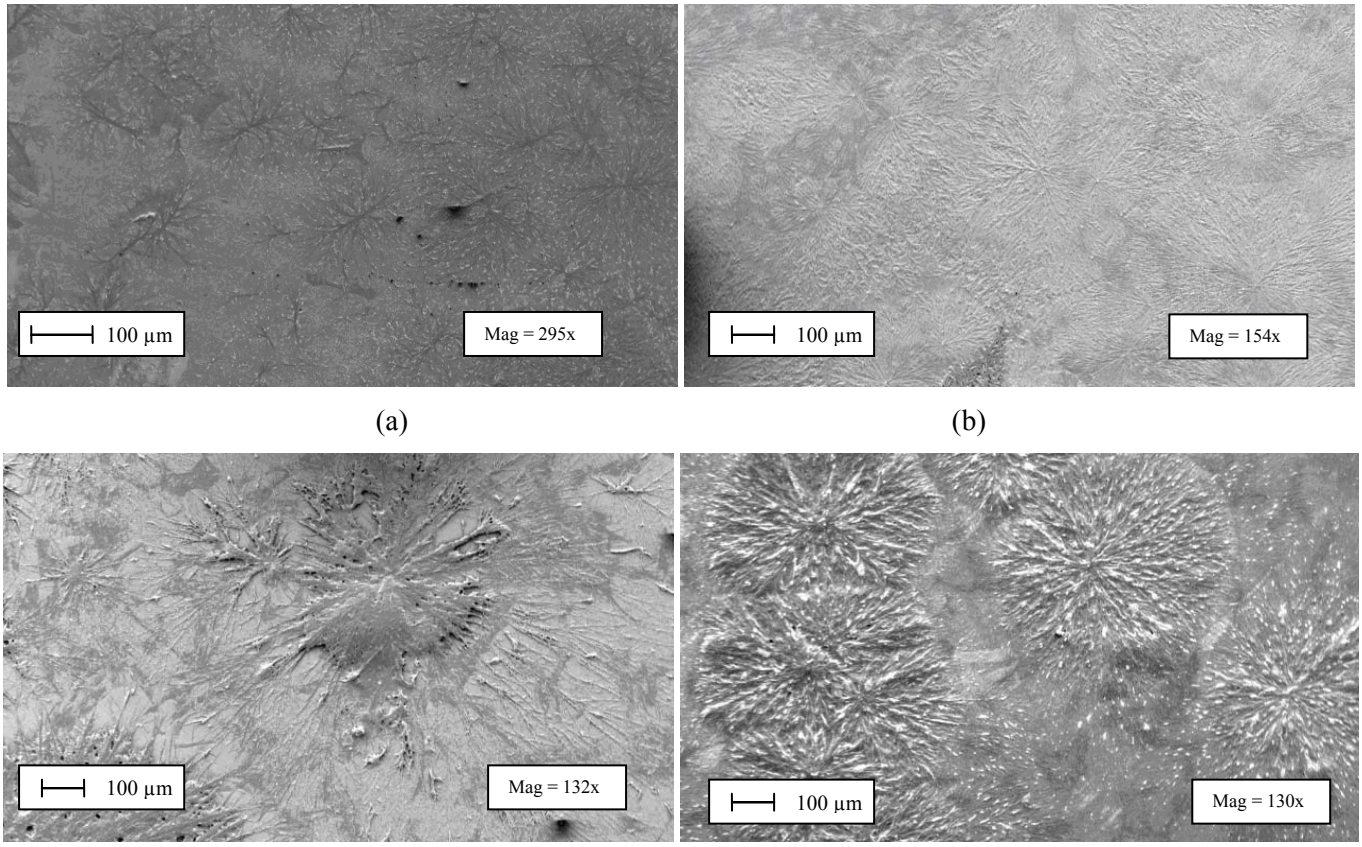

Figure 10 – SEM micrographs of Au coated samples after 4 days incubation for CO_2 laser-patterned samples (a) CT50, (b) CT100, (c) CH50 and (d) CH100.

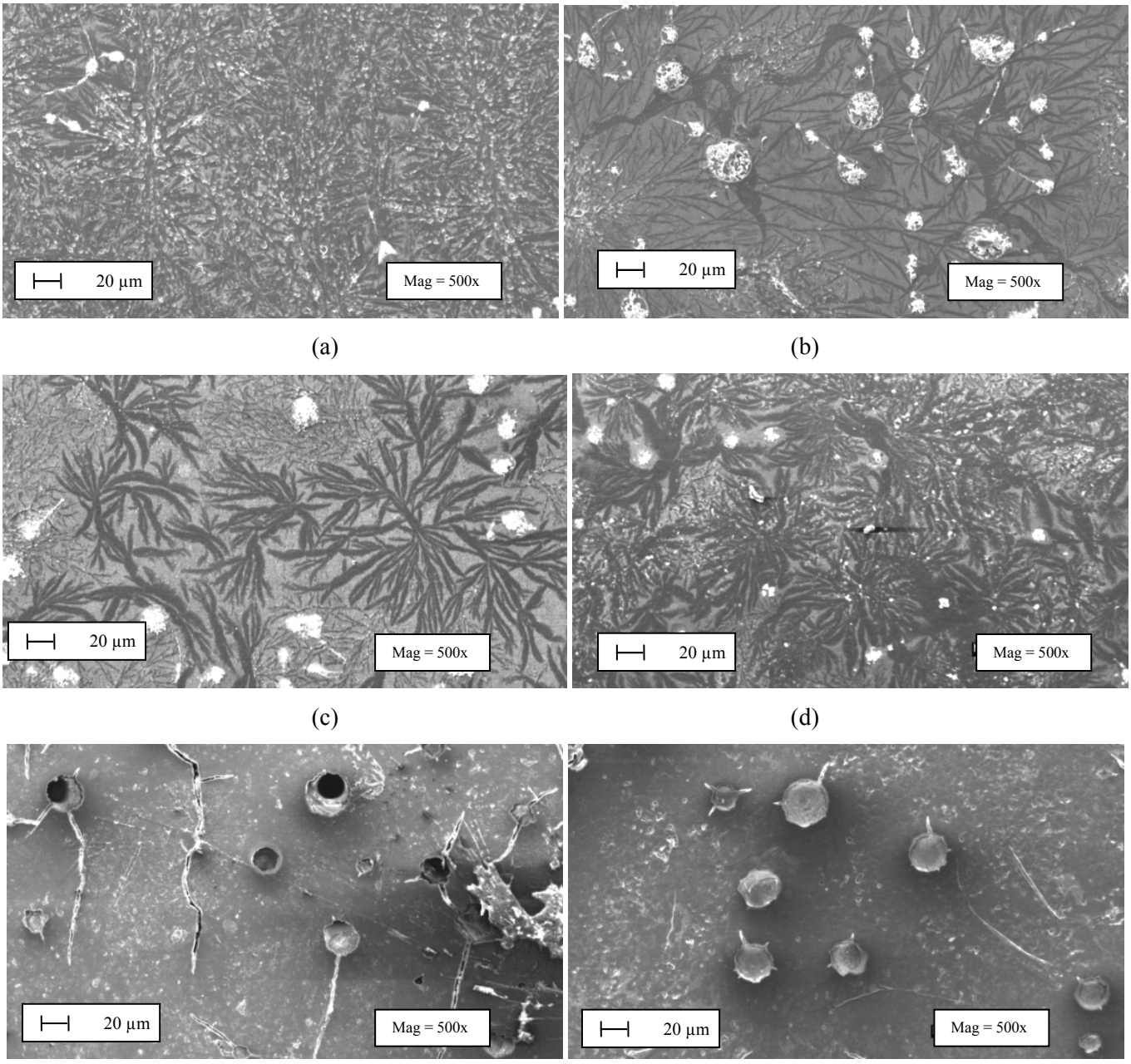

Figure 11 – SEM micrographs of Au coated samples after 4 days incubation for CO_2 laser whole area processed samples (a) CWA17, (b) CWA26, (c) CWA34, (d) CWA51, (e) CWA102 and (f) CWA128.

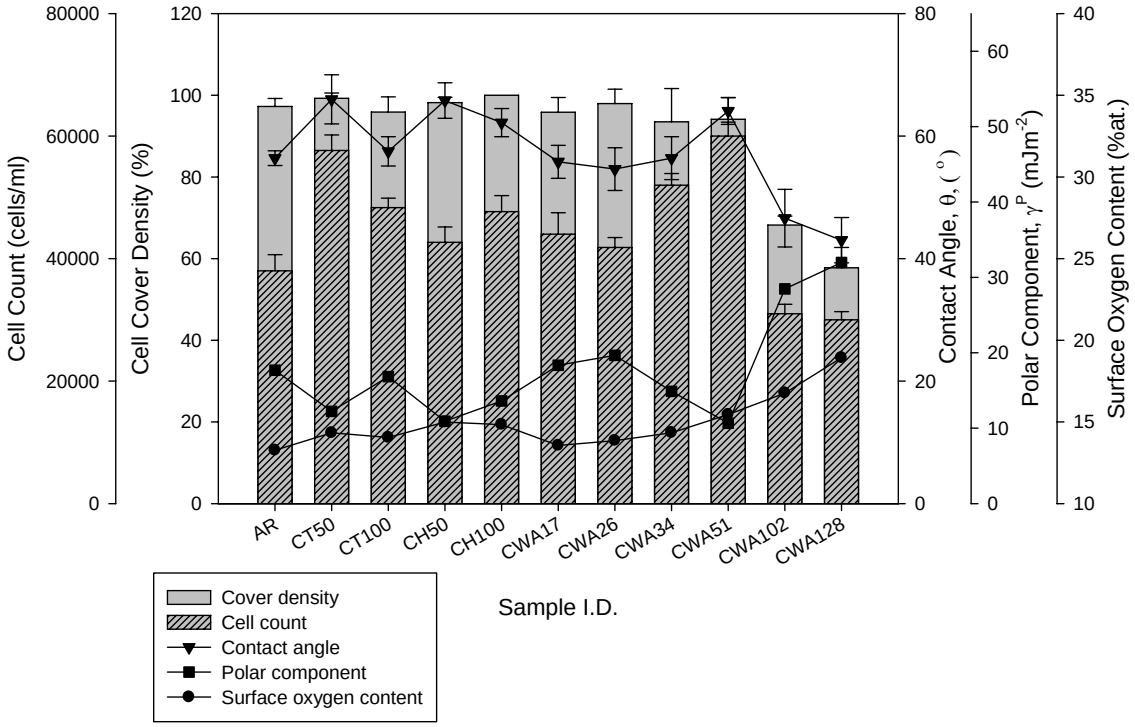

Figure 12 – Cell cover density for each of the CO_2 laser processed nylon 6,6 samples 4 days after incubation.

Table 1 – Results summary for all samples showing roughness parameters, surface oxygen content and wettability characteristics following CO_2 laser processing of nylon 6,6.

Sample ID	*Sa* (*μm*)	*Ra* (*μm*)	*Polar Component, γ^P* (*mJm^{-2}*)	*Dispersive Component, γ^D* (*mJm^{-2}*)	*Total Surface Energy, γ^T* (*mJm^{-2}*)	*Surface Oxygen Content* (*%at.*)	Contact Angle (°)
AR	0.126	0.029	17.69	29.66	47.34	13.26	56.4±1.2
CO_2 Laser-Induced Patterned Samples							
CT50	0.636	0.148	12.24	28.63	40.87	14.33	66.0±4.0
CT100	0.297	0.185	16.86	29.83	46.69	14.05	57.5±2.4
CH50	0.423	0.103	10.93	31.64	42.58	14.99	65.8±2.9
CH100	0.326	0.155	13.63	30.37	44.00	14.84	62.2±2.3
CO_2 Whole Area Irradiative Processed Samples							
CWA17	0.111	0.060	18.36	28.75	47.11	13.56	55.8±2.7
CWA26	0.100	0.158	19.67	28.35	48.02	13.86	54.6±3.5
CWA34	0.101	0.092	14.89	38.55	53.43	14.34	56.4±3.5
CWA51	0.341	0.139	10.66	38.59	49.26	15.45	64.1±2.2
CWA102	4.356	1.236	28.49	23.82	52.31	16.77	46.6±4.7
CWA128	3.201	1.335	31.98	22.78	54.76	18.93	43.0±3.7